JTTEE5 14:330-334
DOI: 10.1361/105996305X59332
1059-9630/$19.00 © ASM International

Interface Material Mixing Formed by the Deposition of Copper on Aluminum by Means of the Cold Spray Process

Victor K. Champagne, Jr., Dennis Helfritch, Phillip Leyman, Scott Grendahl, and Brad Klotz

(Submitted March 3, 2004; in revised form August 28, 2004)

The objective of this article is to present microstructural evidence of a bonding mechanism between copper, which has been deposited by the cold spray process, and an aluminum substrate. Deposition conditions are varied to determine their effects on the nature of the bond. Mechanical measurements, such as adhesion strength and hardness, as well as visual methods are used to characterize the process. A ballistic model is proposed to explain the process.

Keywords bond strength, coatings, cold spray

1. Introduction

Cold spray is a process whereby metal powder particles are used to form a coating by means of ballistic impingement upon a suitable substrate. The metal powders range in particle size from 5 to 50 μm and are accelerated by injection into a high-velocity stream of gas. A converging-diverging nozzle is used to expand preheated gas to supersonic velocity, with an accompanying decrease in temperature (Ref 1-3). The term "cold spray" has been used to describe this process because of the relatively low temperatures (i.e., 273-473 K) of the expanded gas particle stream that exits the nozzle. The adhesion of the metal powder to the substrate, as well as the cohesion of the deposited material, is accomplished in the solid state. The characteristics of the cold spray deposit are quite unique, having significant advantages over other thermal spray methods. The process does not use thermal energy to melt the particles to be deposited but instead relies upon the supersonic impact of the particles on the substrate, which plastically deforms and causes cratering. The bonding mechanism was theorized to be analogous to that of explosive welding, in which the formation of a solid-state jet of metal occurs at the impact point between the particle and the substrate (Ref 4, 5).

2. Experimental Procedure

To demonstrate the nature of the metallic bond created by the cold spray process, the effect of spray parameters on the copper-aluminum bond was investigated. The system used for this work is described by Fig. 1. High-pressure (2-3.5 MPa) nitrogen is distributed to a gas heater and powder feeder. The main gas stream passes through electrically heated tubing that heats the gas to 573 to 773 K. A Praxair model 1264HPHV high-pressure (Appleton, WI), high-volume powder feeder provides controlled metering of the powder into the powder gas stream. These two gas streams are combined in a manifold that is set immediately before the nozzle. The particles are subsequently accelerated to supersonic speeds via the converging-diverging nozzle design. The gas control module, gas heater, and the powder feeder are interfaced via Ethernet connections to a computer control system to control the temperature and pressure of the gas streams in addition to the powder feed rate. The computer control system provides not only real-time monitoring of these parameters, but the data are continuously collected and stored, and are available for subsequent analysis. The spray nozzle motion is controlled by a fully programmable Motoman UP20 six-axis robotic system (West Carrollton, OH).

The substrate material used in this study was 6061 aluminum. A spherical copper powder (500A) from ACuPowder International LLC (Union, NJ) with an average particle size of 17 μm and 99.85 purity was used to generate the coatings. The compositions of the 6061 aluminum substrate and the copper powder are given in Table 1.

The 500A copper powder was examined with a Hitachi (Tokyo, Japan) S4700 field emission scanning electron microscope (FSEM). Specimens were prepared by sprinkling the powder on wet carbon paint and gently blowing the excess powder from the surface. After the paint dried, the specimens were examined under the microscope. The particles in Fig. 2 are seen to be quite spherical and relatively uniform.

A Horiba LA-910 laser-scattering particle size distribution analyzer (Irvine, CA) was used to determine the size distribution of the powder. This technique used laser scattering from the particles suspended in solution to determine the distribution. Several measurements were made on the sample. In general, the measurements agreed with each other, and a representative measurement is shown in Fig. 3.

Because the bonding mechanism was theorized to be analogous to explosive bonding, conventional means of testing bond strength were avoided because the bond strength might exceed that of the glues used for standard tensile strength measurements (i.e., 70-80 MPa). Therefore, an alternative method for determining the bond strength was used. The triple-lug shear test

Victor K. Champagne, Jr., Dennis Helfritch, Phillip Leyman, Scott Grendahl, and **Brad Klotz,** U.S. Army Research Laboratory, Weapons and Materials Research Directorate, Aberdeen Proving Ground, MD 21005-5069. Contact e-mail: vchampag@arl.army.mil.

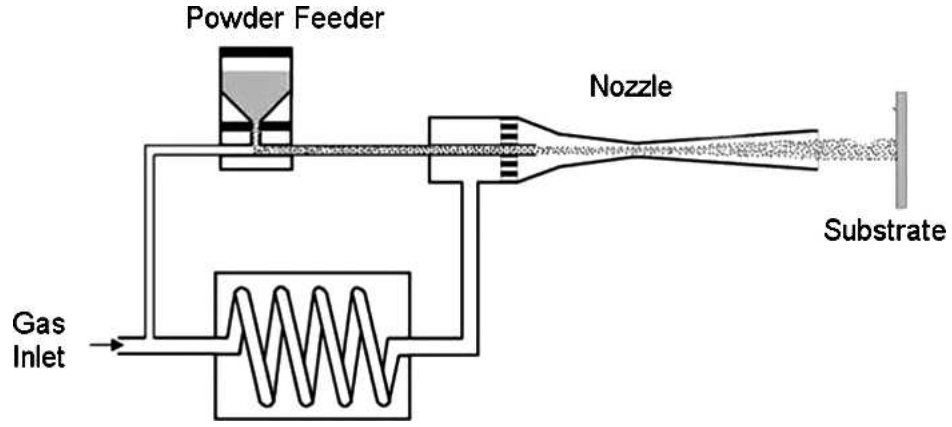

Fig. 1 Schematic of the Army Research Laboratory cold spray system

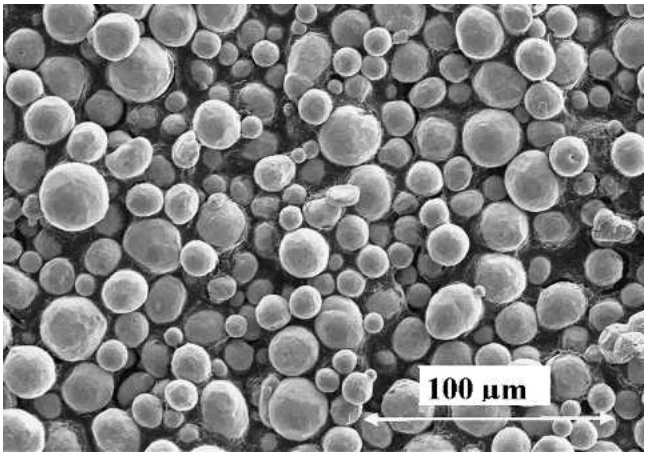

Fig. 2 FSEM photograph of copper powder

Table 1 Typical chemical composition (wt.%) of materials

Elements	6061 Aluminum	500A Copper powder
Aluminum	Balance	<0.005
Chromium	0.04-0.35	<0.005
Copper	0.15-0.4	99.85
Iron	0-0.7	0.005
Magnesium	0.8-1.2	<0.005
Manganese	0.15 max	<0.005
Silicon	0.4-0.8	<0.005
Titanium	0.15 max	…
Zinc	0.25 max	0.01

method, which was specifically designed for bimetallic joints formed by roll-bonding and explosive-bonding processes, was used to determine the adhesion of the copper coating to the aluminum substrate. The triple-lug procedure for the test method was prescribed in military specification MIL-J-24445A (Ref 6). The procedure called for strips of the coating to be sheared off the substrate by forcing the coating/substrate past a sharp corner. The force required to shear off the coating and the coating/substrate attachment area then yielded the shear strength of the bond. This arrangement is shown in Fig. 4.

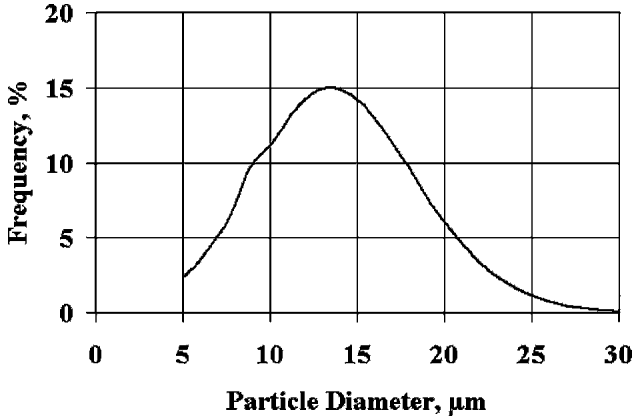

Fig. 3 Copper powder size distribution (Horiba LA-910)

The aluminum substrates were placed 15 to 35 mm from the nozzle exit aperture and were coated with copper to ~2 mm in thickness using the process parameters listed in Table 2. Nitrogen was the carrier gas in all tests. The powder carrier gas was maintained at 70 to 140 kPa greater than the heated gas. An area covering 4.7 × 3.8 mm of the aluminum block was coated in a raster pattern at the specified traverse speed, with an index of 1.0 mm between passes. Two levels of each variable were used to evaluate the effect of each of the parameters on coating hardness and bond strength. The coatings were machined flat and smooth to a 1.5 mm thickness, utilizing a milling machine prior to hardness testing. The copper material between the three lugs was removed, leaving the aluminum surface.

Hardness measurements were performed on the coatings using a Wilson Instruments model C524-T Rockwell hardness tester (Norwood, MA). Nine measurements were taken in a 19 mm diameter circular pattern on each coating. The Rockwell B tests used a 1.587 mm ball at a 100 kg major load and a 10 kg minor load.

The stress-to-shear failure tests were performed on an Instron 8500 Plus Dynamic Testing System (Norwood, MA) equipped with an Instron model 1331 load frame and controlled by a Series IX automated computer program. The aluminum block with the three machined rectangular lugs was inserted into the fixture. The fixture then was placed in the Instron load frame, and a cali-

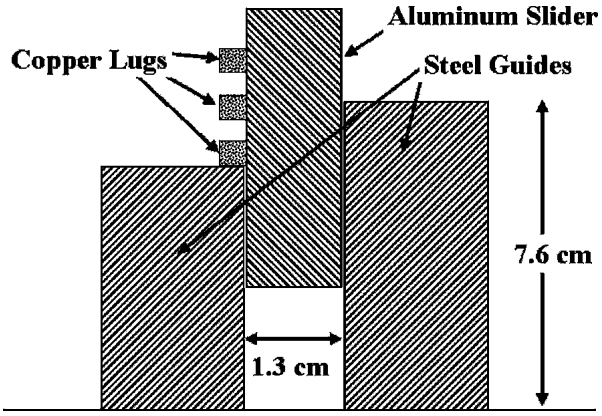

Fig. 4 Schematic of the shear test fixture using military specifications MIL-J-24445A

Table 2 Deposition parameters and coating thickness

	Trial			
Parameters	**1**	**2**	**3**	**4**
Feed rate, kg/s × 10^4	1	4	4	1
Main gas pressure, MPa	1.93	1.93	2.62	2.62
Delta gas pressure, kPa	140	70	70	140
Temperature, K	723	623	723	623
Standoff distance, mm	35	15	35	15
Traverse speed, mm/s	50	50	10	10
Coating thickness, mm	1.02	1.02	1.14	1.09

Table 3 Rockwell B hardness test results for copper coatings

Trial (Table 2)	Average, kPa	SD
1	490	0.9
2	529	1.83
3	482	0.61
4	465	1.02

Table 4 Results of the triple-lug bond strength tests

Trial (Table 2)	Load at failure, N	Shear strength, MPa
1	4462	36.87
2	5067	41.86
3	5574	46.08
4	8389	69.34

brated downward load was used to stress each lug to failure at the copper-aluminum interface.

3. Results

The average hardness for each coating is reported in Table 3.

Table 4 gives the average shear strength of each triple-lug set deposited under the deposition conditions given by Table 2. The test samples displayed a cohesive failure within the copper coating and not an adhesive failure at the interface between the copper coating and the aluminum substrate. This occurred in all of the samples sheared.

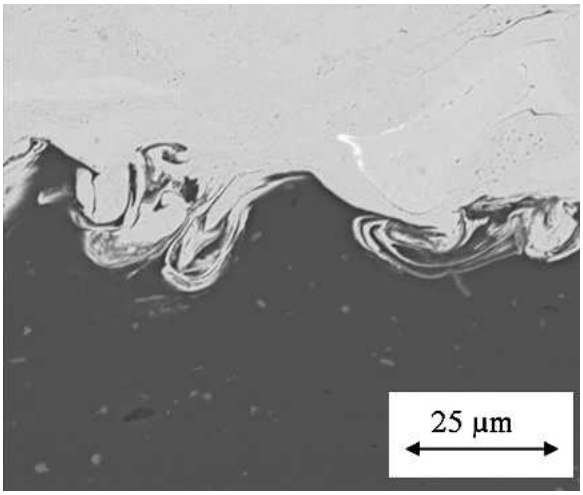

Fig. 5 EDS image of a copper coating on aluminum

The coating that yielded the highest shear strength was trial No. 4, which was deposited at the higher nitrogen gas pressures for both the main gas and the powder gas but at the lower conditions for all remaining parameters. Specifically, a coating with higher shear strength was produced when the copper powder was fed at a lower feed rate (i.e., 1×10^{-4} kg/s), accelerated at a gas pressure of 2.62 MPa and a gas temperature of 623 ° K, while the nozzle was close to the substrate and was traversing at a relatively slow speed.

Cross sections of the copper coatings were prepared for metallographic examination. Samples were sectioned with a diamond cut-off saw. To avoid contamination, diamond polishing media and diamond suspension were used throughout the grinding, rough polishing, and final polishing steps.

Energy-dispersive spectrometry (EDS) was used to investigate the interface between the copper deposit and the aluminum substrate to determine the extent of mixing. Metallographic cross sections were used for this analysis. Figure 5 shows the EDS image. As denoted, the darker region is the aluminum substrate, and the lighter areas are the copper deposit. There is clear evidence of forced mixing between the deposited copper and the aluminum substrate, demonstrating the tenacious nature of the bond between the copper and the aluminum.

4. Discussion

The bonding mechanism between particles and substrate and between particles and previously deposited particles created by the cold spray process was caused by substrate penetration, interfacial heating, and liquid jet formation resulting from high-velocity impact. These phenomena are described by Fig. 6, in which the behavior of a single particle impacting a substrate is modeled (Ref 7). The computation uses the Zerilli-Armstrong (strain-rate dependent) and the Steinberg-Guinan-Lund plastic models, respectively, for copper particles impacting an aluminum plate. In this case, a 20 μm copper sphere impacting an

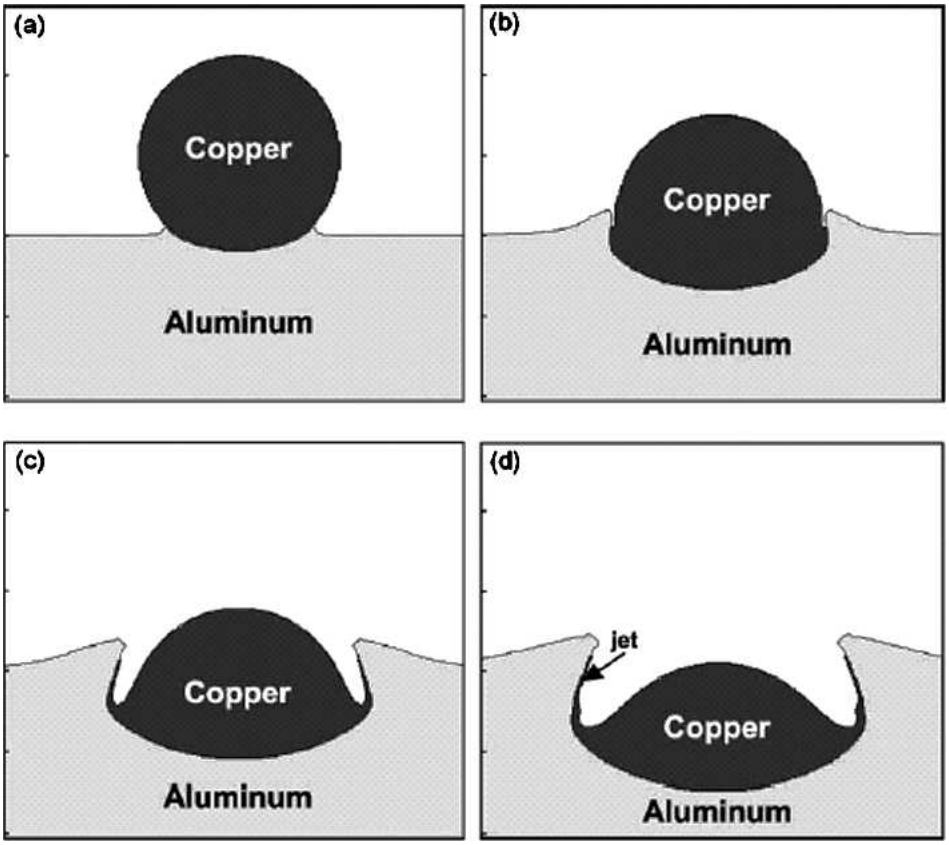

Fig. 6 Impact of a copper particle on a copper substrate at successive times: (a) 5 ns, (b) 20 ns, (c) 35 ns, and (d) 50 ns

aluminum plate at 650 m/s is modeled. The frames show the impact at successive times: (Fig. 6a) 5 ns; (Fig. 6b) 20 ns; (Fig. 6c) 35 ns; and (Fig. 6d) 50 ns. Because the calculation shows that the interfacial pressure and the von Mises equivalent stress are considerably higher than the zero plastic-strain yield strength of copper and aluminum, it is appropriate to treat the material adjacent to the interface as a viscous "fluid-like" material. The viscous, fluid-like nature of the jet can be expected to result in the formation of interfacial waves, roll-ups, and vortices.

The interface development can be simply described through empirical particle-substrate relationships. The thorough mixing shown by Fig. 5 can only be achieved through deep-impact penetration of the copper into the aluminum. An empirical projectile penetration law by Eichelberger and Gehring (Ref 8) relates the crater volume (in cubic meters) produced by micrometeoroid impact on spacecraft. This is given by the equation:

$$\text{Volume} = \frac{(4 \times 10^{-5})E}{B} \qquad \text{(Eq 1)}$$

where E is the particle kinetic energy in joules and B is the substrate Brinell hardness number. It was shown (Ref 9) that this equation yielded accurate results for velocities below 10 km/s.

To make use of Eq 1, we substitute $1/2(4/3\pi r^3\rho)V^2$ for E, where ρ is the particle density given in kilograms per cubic meter, r is the particle radius in meters, and V is the particle velocity in meters per second. We assume that the crater volume is the particle face area (πr^2) times the penetration depth. Thus, Eq 1 becomes:

$$\text{Volume} = (\pi r^2)L = \frac{(4 \times 10^{-5})(1/2)(\rho 4/3\pi r^3)V^2}{B} \qquad \text{(Eq 2)}$$

The penetration depth, L (in meters), is then given:

$$L = (4 \times 10^{-5})\left(\frac{2\rho r}{3}\right)\left(\frac{V^2}{B}\right) \qquad \text{(Eq 3)}$$

If we assume that the onset of thorough interfacial mixing occurs when particles are completely embedded at $L = 2r$, we can solve for the onset velocity:

$$V = \left[(7.5 \times 10^4)\left(\frac{B}{\rho}\right)\right]^{0.5} \qquad \text{(Eq 4)}$$

Equation 4 gives us a simple, empirical method to estimate the particle velocity needed for the attainment of interfacial mixing. For copper particles impacting 6061 aluminum, Eq 4 gives an onset velocity of 500 m/s. The actual particle velocities used during the creation of the sample in Fig. 5 are shown in Fig. 7. These velocities were measured by a TECNAR Automation Ltd. DPV-2000 (St-Hubert, Quebec, Canada), dual-slit, laser-illuminated optical sensor. This Fig. 7 shows the particle veloc-

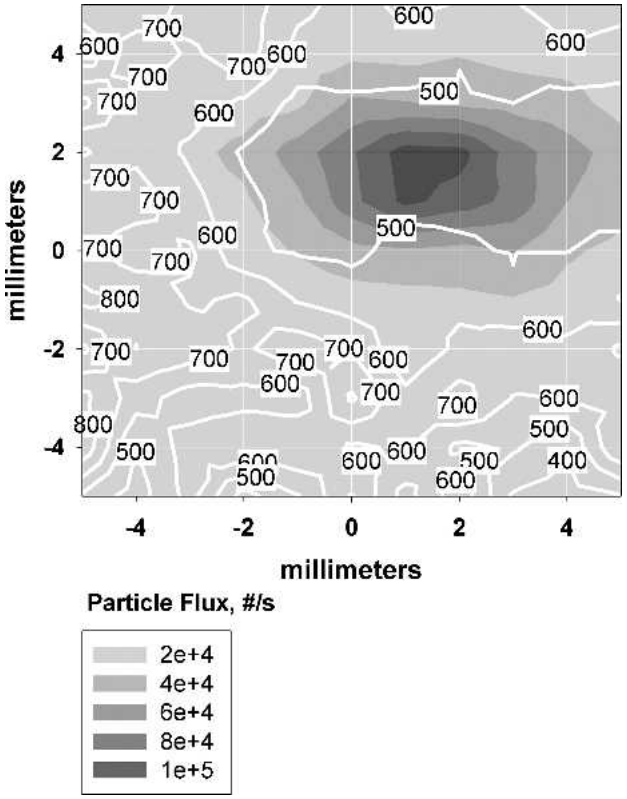

Fig. 7 Nozzle plume particle velocity and flux distributions

ity and flux distributions in a plane perpendicular to the nozzle axis, 2.5 cm downstream of the nozzle exit. The particle velocity is indicated by constant velocity contours, and the particle flux density is indicated by background darkness. The plume centerline is seen to be at the coordinates $x = 1$ mm, $y = 1.5$ mm. It is seen that the majority of the plume particle flux is contained by the 500 m/s isoline. Higher velocities are also indicated but apply to a relatively small number of particles. The conditions for the creation of a well-mixed interface are clearly satisfied.

5. Conclusions

- The cold spray process can yield an exceptionally strong bond between copper and Al 6061.
- High-velocity impact can yield viscous mixing at the copper particle-aluminum substrate interface.
- The resulting bond exhibited shear resistance at the interface greater than the shear strength of the copper coating.
- An empirical model shows that interface mixing depends on substrate hardness and coating material density.

The coatings deposited by the cold spray process demonstrated exceptionally strong bonds caused by high-impact forces. These coatings were generated without high temperatures, resulting in significantly reduced, thermally generated internal stresses.

References

1. A. Papyrin, Cold Spray Technology, *Adv. Mater. Proc.,* (September), 2001, p 49-51
2. R. McCune, W. Donlon, O. Popoola, and E. Cartwright, Characterization of Copper Layers Produced by Cold Gas-Dynamic Spraying, *J. Thermal Spray Technol.,* Vol 9 (No. 1), 2000, p 73-82
3. T. Stoltenhoff, H. Kreye, and H. Richter, An Analysis of the Cold Spray Process and Its Coatings, *J. Thermal Spray Technol.,* Vol 11 (No. 4), 2002, p 542-550
4. V. Radic, The State of Two-Metal Contact Boundary at High-Velocity Impact, *The Scientific Journal FACTA UNIVERSITATIS Series: Mechanical Engineering,* Vol 1 (No. 8), 2001, p 1017-1023
5. W. de Rosset, "Explosive Bonding of Refractory Metal Liners," Report ARL-TR-3267, Army Research Laboratory, Aberdeen Proving Ground, MD, August, 2004
6. MIL-J-24445A, "Joint, Bimetallic Bonded, Aluminum to Steel," Department of Defense Military Specification, March 1, 1971
7. M. Grujicic, J. Saylor, D. Beasely, W. DeRosset, and D. Helfritch, Computational Analysis of the Interfacial Bonding between Feed-Powder Particles and the Substrate in the Cold-Gas Dynamic-Spray Process, *Appl. Surf. Sci.,* Vol 219 (No. 3-4), 2003, p 211-227
8. R.J. Eichelberger and J.W. Gehring, Effects of Meteoroid Impacts on Space Vehicles, *ARS J.,* Vol 32 (No. 10), 1963, p 1583
9. R.L. Bjork, "Review of Physical Processes in Hypervelocity Impact and Penetration," Rand Corporation Memorandum RM-3529-PR, U.S. Air Force Contract AF 49(638)-700, 1963